RSC Advances

ROYAL SOCIETY
OF CHEMISTRY

www.rsc.org/advances

1   **Cross-linked Reverse Micelles with Embedded Water Pools: A Novel Catalytic**

2   **System Based on Amphiphilic Block Copolymers**

3   Ruihan Liu[a], Shiping Wang[b], Jia Yao[a,*], Weiwei Xu[a], Haoran Li[a]

4   [a] State Key Laboratory of Chemical Engineering, Department of Chemistry, Zhejiang

5   University, Hangzhou 310027, PR. China

6   [b] Key Lab of Applied Chemistry of Zhejiang Province, Department of Chemistry,

7   Zhejiang University, Hangzhou 310027, PR. China

8   **Abstract**

9   Based on the idea of structural design, a novel catalytic system from a block

10   copolymer for the oxidation reaction of 2,3,6-trimethylphenol (TMP) was developed.

11   The block copolymer, poly(4-vinylpyridine)- block -poly(ethylene glycol)- block

12   -poly(4-vinylpyridine) (P4VP-PEG-P4VP), was synthesized via anionic polymerization.

13   After self-assembly in water/1-hexanol solution and shell crosslinking, the block

14   copolymer formed the shell cross-linked reverse micelles (SCRMs). The $CuCl_2$

15   complexed SCRMs were used in the catalytic oxidation reaction of TMP. Through

16   coordinating with metal ions and regulating the distribution of metal catalytic active

17   centers, and with the co-catalysis effect of the immobilized water droplets, this

18   polymer-supported catalyst system demonstrated an efficient catalytic activity and

19   recoverability. This work provides not only a promising catalyst based on mesoscale

20   structure design using block copolymers, but also an example for deeper understanding

21   on the structure effect in catalysis.

22

23   **Keywords:** Amphiphilic block copolymer; P4VP-PEG-P4VP; Catalyst for oxidation

24

25   [*] **Corresponding author:** Department of Chemistry, Zhejiang University, Hangzhou

26   310027, PR China.

27   E-mail addresses: yaojia@zju.edu.cn (Jia Yao)

28

1 **Introduction**

2 Over the recent years, the development of polymer-supported catalysts[1-4] has
3 attracted widespread attention, with consideration of the structure at nanoscopic or
4 mesoscopic levels[5-8], offering a viable method for catalyst design. The designed
5 catalysts can dramatically alter their reactivity, selectivity, and efficiency, by impacting
6 the location and activity of catalytic active centers. But designing a more effective
7 polymer-supported catalyst with a specific structure is still a challenge, because of the
8 lack of the knowledge in correlation the reaction mechanism and the mesoscale
9 structure.

10 The micelles from amphiphilic block copolymers have already been developed in
11 catalysis applications[9-11]. Generally micelles are considered to have a hydrophobic core
12 and a hydrophilic shell in polar solvents. Yet if the solvent system is less hydrophilic,
13 the core and the shell may be inverted to give reverse micelles (RMs)[12, 13]. Additionally,
14 compared with the self-assembled micelles formed through noncovalent interactions,
15 the formation of shell cross-linked reverse micelles (SCRMs)[7, 14-16] can provide
16 reinforcement and stability whatever the environmental conditions change.

17 The catalytic oxidation of TMP using molecular oxygen as oxidant is a key step to
18 synthesize vitamin, pharmaceuticals, and flavors in chemical industry[17]. The
19 homogeneous copper catalyst system can achieve high conversion and selectivity[18-20],
20 but a serious drawback is that almost or even more than a stoichiometric amount of
21 catalyst is required, which is environmenental unfriendly. Polymer supported metal
22 catalysts[21-24] are considered as more friendly to the environment. Takaki et al.[25]
23 succeeded in an oxidation of TMP with polymer-supported copper catalysts. But it took
24 a long time to complete the reaction and the products could be obtained just under high
25 O_2 pressure (10 atm). The relatively low activity might be due to the simple structure of
26 Takaki's catalyst. Hence, in this paper a novel catalyst system was designed for the
27 oxidation of 2,3,6-trimethylphenol (TMP) by dioxygen. The catalyst carrier is a kind of
28 cross-linked reverse micelle formed by self-assembly of block copolymers, with a water
29 pool encapsulated. The relationship between the mesoscale structure and the catalysis
30 efficiency was investigated. It is worth mentioning that a small amount of water can act
31 as the activator in some catalytic reactions[26, 27], so the structure of the aqueous cores of

1   RMs, even with water pools embedded in, maybe have a positive effect on promoting

2   reactions.

3   To prepare the SCRM structure, in this work, an ABA amphiphilic block copolymer

4   poly(4-vinylpyridine)-block-poly(ethylene   glycol)-block-poly(4-vinylpyridine)

5   (P4VP-PEG-P4VP) was synthesized via anionic polymerization. P4VP-PEG-P4VP

6   formed RMs in a mixed bi-phase solution (Scheme 1). The hydrophilic core of

7   P4VP-PEG-P4VP RM consists of PEG blocks, enclosing a water pool, and the P4VP

8   blocks constitute the shell. 1,2-bis(2-iodoethoxy) ethane (BIEE) was used as a

9   cross-linking agent to selectively quarternize the nitrogen atoms on the pyridine groups

10   in the micelle shell, thus formed SCRMs. Through the coordination with metal ions[28-34],

11   CuCl$_2$-(P4VP-PEG-P4VP) SCRMs were successfully applied in the catalytic oxidation

12   reaction of TMP in the 1-hexanol media, followed by reuse of the catalyst in several

13   cycles.

14

Experimental section

Materials

17   Poly(ethylene glycol) (PEG, M_n = 2000 g/mol, Aldrich) was dried under vacuum at

18   55 °C for 1 h, and then stored under nitrogen at -15 °C. 4-Vinylpyridine (4VP, Aldrich)

19   was passed through an activated basic alumina column to remove the stabilizing agents,

20   stirred with a small amount of CaH$_2$ overnight at room temperature, followed by

21   vacuum distillation. 4VP was filled with nitrogen and stored in a refrigerator at -15 °C.

22   Tetrahydrofuran (THF) was dried by being refluxed over sodium and distilled in

23   nitrogen atmosphere right before use. Potassium naphthalene was prepared by

24   dissolving naphthalene in dried THF and refluxing the solution over potassium until it

25   became dark blue. The feed ratio of potassium and naphthalene was 1:1.

26   2,3,6-Trimethylphenol was donated by Zhejiang NHU Company Ltd. All the other

27   reagents and solvents were of analytical grade from Aldrich and were used without

28   further purification.

29

Synthesis of P4VP-PEG-P4VP

31   2.0 g dried PEG was dissolved in 100 mL dried THF, and the solution was transferred

32   to a 250 mL round-bottomed flask under nitrogen. 4 mL freshly prepared solution of

1   potassium naphthalene in THF (0.5 mol/L) was injected into the round-bottomed flask

2   via a nitrogen-washed injector, and stirred until the color of solution changed to light

3   green. The mixed solution was stirred at room temperature for 0.5 h to form the

4   alcoholate macroinitiator. A known amount of freshly distilled 4VP was then charged to

5   the reactor under nitrogen atmosphere at -78 °C. Polymerization was carried out at this

6   temperature for 24 h. The crude copolymer was dissolved in ethanol at 60 °C and

7   precipitated at room temperature. The copolymer was dissolved in ethanol at 60 °C

8   again, and then transferred to a dialysis tube to dialyze against water for 1 week to

9   remove   small   molecules.   The   diblock   copolymer,   poly(ethylene

10 glycol)-block-poly(4-vinylpyridine) (P4VP-PEG), was synthesized using a similar

11 method for comparison.

12

13 **Self-assembly and shell cross-linking of P4VP-PEG-P4VP reverse micelles**

14   Water was added into 1-hexanol to reach water content of 50%, forming 100 mL

15 bi-phase mixed solution. Then the block copolymer P4VP-PEG-P4VP was added to the

16 solution at pH 4 (polymer weight: 0.15 %) and stirred at room temperature for 24 h.

17   1 mmol BIEE was dissolved in 10 mL 1-hexanol. After being stirred and standing for

18 24 h, the BIEE solution was added into the above P4VP-PEG-P4VP solution drop by

19 drop, to achieve shell cross-linking. The solution was then stirred at low speed for at

20 least 3 days at room temperature. Several degrees of cross-linking were studied, among

21 which the highest was 30%. The solvent was stripped by freeze-drying and the SCRMs

22 dried powder was obtained.

23

24 **Preparation of the $CuCl_2$-(P4VP-PEG-P4VP) SCRMs complex**

25   0.5 mmol P4VP-PEG-P4VP SCRMs were dissolved in 100 mL 1-hexanol. Solution

26 of the appropriate amount of the copper salts ($CuCl_2 \cdot 2H_2O$, Aldrich) in 10 mL

27 1-hexanol was slowly added, and then the combined solution was mixed under

28 moderate stirring for 12 h. Products were obtained by centrifugation, washing and

29 freeze-drying.

30

31 **Oxidation of TMP by O_2 using $CuCl_2$-(P4VP-PEG-P4VP) as catalyst**

1   Catalytic oxidation of TMP was conducted in all-glass reactor vessels consisting of a

2   50 mL round bottomed flask connected reflux condensing tube and ventilation capillary.

3   TMP (136.2 mg, 1 mmol) was dissolved in 1-hexanol (20 mL), and stirring continued at

4   room temperature under O_2 (1 atm). After the addition of an appropriate amount of H_2O

5   into the $CuCl_2$-(P4VP-PEG-P4VP) SCRMs complex, the complex morphological

6   characteristic   changed   from   powder   to   paste.   The   catalyst,   moist

7    $CuCl_2$-(P4VP-PEG-P4VP) SCRMs, was added to the TMP solution and the mixture was

8   stirred under the conditions indicated in Table 1 which was monitored by gas

9   chromatograph (GC). The precipitated catalyst was recovered through centrifugation

10   and thorough washes in 1-hexanol. After being dried by lyophilization and wetted again,

11   the catalyst was reused in the next cycle (Table 2).

12

13   **Characterization methods**

14   Transmission electron microscope (TEM) was performed on a Hitachi HT-7700 at an

15   acceleration voltage of 120 kV. A drop of very dilute solution was applied onto a

16   carbon-coated TEM copper grid. The sample was then immediately frozen by liquid

17   nitrogen and dried by lyophilization.

18   Dynamic light scattering (DLS) measurements were performed on Malvern Zetasizer

19   Nano-ZS equipped with a He-Ne laser at a wavelength of 633 nm. The experimental

20   data were analyzed by the CONTIN method which is based on an inverse-Laplace

21   transformation of the data and provides access to a size distribution histogram for the

22   analyzed micellar solutions. The ζ potential of RM nano-particles was determined by

23   laser Doppler anemometry using a Malvern Zetasizer Nano-ZS. The temperature was

24   set to 25 °C and the results were normalized with respect to the polystyrene standard

25   solution.

26   The coordination of Cu (II) and SCRMs was measured by Electron paramagnetic

27   resonance (EPR) on Bruker A300 with X-band frequencies at 108 K. The solution of

28   10^{-4} M copper-containing SCRMs in DMSO was transferred to an EPR tube and

29   shock-frozen in liquid nitrogen to obtain a transparent, glassy sample.

30   The yields of all products obtained from TMP oxidation, were determined by GC

31   (Agilent GC-2014) using ethyl benzoate as internal standard.

32

Results and discussion

Synthesis and characterization of P4VP-PEG-P4VP amphiphilic block copolymer

P4VP-PEG-P4VP was synthesized by anionic polymerization in THF at -78 °C using potassium naphthalene as the initiator. Vamvakaki et al.[35] synthesized the poly(ethylene oxide-tertiary amine methacrylate) with the potassium naphthalene as a functional initiator. In our study, anionic polymerization was initiated with potassium naphthalene from PEG, and P4VP-PEG-P4VP was obtained by the polymerization of 4VP in a controlled mechanism (Scheme 2).

Analysis of the polymer including ^{1}H NMR and GPC can be found in ESI Figure S1–S2. The ratio of polymer to monomer and the number-average molecular weight could be calculated through ^{1}H NMR spectrum. Based on the calculation of the NMR spectrum, we found that one P4VP-PEG-P4VP chain had 45 EG units and 50 4VP units, with a $M_{copolymer}$ of 7200 g/mol. The M_n values obtained from NMR and GPC measurements were consistent.

Formation of P4VP-PEG-P4VP SCRMs

The shell cross-linked reverse micelles were prepared in two steps. Firstly, P4VP-PEG-P4VP self-assembled into RMs in water/1-hexanol solution (Scheme 1). Then, the solution of cross-linker BIEE was added into the micelle solution under stirring condition (Scheme 3), forming P4VP-PEG-P4VP SCRMs.

In the first step, the mixed solution of water/1-hexanol was used as media for P4VP-PEG-P4VP RMs self-assembly at acidic condition. As water is a good solvent for the PEG block but not for the P4VP block, the formed core-shell RMs had PEG chains as the core and P4VP chains as the shell. The morphologies of the copolymer self-assemblies were characterized by TEM.

For comparison, P4VP-PEG self-assemblies were prepared under the same conditions as described in the experimental section. As shown in Figure 1a, the P4VP-PEG diblock copolymer self-assembled into vesicles with a large outside diameter of about 2 μm which were loose and unstable. P4VP-PEG-P4VP formed core-shell RMs, partially with a hollow structure (actually a water pool) (Figure 1b). The folding of the ABA copolymer chain of P4VP-PEG-P4VP enhanced the rigidity of the shell, providing P4VP-PEG-P4VP micelle with a higher stability than P4VP-PEG micelle. The

1   P4VP-PEG-P4VP RMs had an average outside diameter of 100 ± 20 nm with a shell

2   thickness of approximately 50 nm.

3   A small amount of $CuCl_2$ was used as staining agent to determine the location of the

4   pyridine group in the RMs. TEM image in Figure 1c indicated that the pyridine groups

5   were located on the shell. The small dots near outside surface were coils of P4VP

6   molecular chain, generated by the coordination of Cu^{2+} and pyridine groups.

7   The size of the water pool in RMs could be controlled by the component ratio of

8   solution[15]. The morphologies of P4VP-PEG-P4VP self-assemblies at different

9   component ratios of solution were illustrated in Figure 2. And ESI Figure S3 showed

10   the particle size distribution of P4VP-PEG-P4VP copolymer self-assemblies according

11   to DLS measurements, and the result is consistent with that obtained from TEM. When

12   using only 1-hexanol, the polymers could not form a stable aggregation. With the ratio

13   of water increasing in the mixture of water/1-hexanol, micelles can form. The ratio of

14   water was higher, the water pool in RMs could form more easily. As the mass ratio of

15   water/1-hexanol reached 1 and above (Figure 2d-e), the core-shell structure micelles

16   could be obtained. As the ratio of water/1-hexanol increased from 1.5 to 4, the water

17   pool inside the RM became bigger. When the solution was pure water, the polymers

18   formed huge thin films.

19   The outside surface properties of P4VP-PEG-P4VP RMs were investigated by

20   measuring ζ potential[36-38], see ESI Figure S4-S5. At a positive potential, the RMs

21   showed a stable structure. With the increase of pH, the potential declined, for the

22   decreasing degree of protonation of P4VP. The ζ potential became negative in the pH

23   region above 5.4 and meanwhile the structure of RMs was not stable.

24   Following self-assembly, BIEE was used to crosslink the shell layer, reinforcing the

25   RM structure through covalent bonding. Scheme 3 describes the formation procedure of

26   P4VP-PEG-P4VP SCRMs. As a cross-linking reagent, BIEE could quarternize the

27   nitrogen atoms on the pyridine group.

28   Therefore, self-assemblies of the P4VP-PEG-P4VP RMs in the mixed solution of

29   water/1-hexanol at a concentration of 2×10^{-4} M were stabilized through crosslinking

30   reactions between the pyridine groups within the peripheral shell. The morphologies of

31   SCRMs with different extent of crosslinking were shown in ESI Figure S6. With the

32   increasing content of crosslinking at the peripheral shell, the binding among

1   P4VP-PEG-P4VP micelles were stronger. At the 30% degree cross-linking, partial

2   peripheral P4VP segments formed the smooth thin film, with interior structures of

3   P4VP-PEG-P4VP micelles located on it separately. The SCRMs maintained spherical

4   and well-dispersed. Additionally, large aggregations of SCRMs could be achieved by

5   increasing the concentration of micelles or BIEE, see in ESI Figure S7.

6

7   **Catalytic application of P4VP-PEG-P4VP SCRMs in oxidation of TMP**

8   To achieve the preferable catalyst for further oxidation of TMP, $CuCl_2 \cdot 2H_2O$ was

9   added to the maximum micelle loading (Cu: 4VP = 1:1) corresponding to pyridine units

10 in the P4VP-PEG-P4VP SCRM solution (0.2 mmol/L). (Note: the concentration of 4VP

11 in the sample was calculated using M_n of P4VP-PEG-P4VP same with the value used

12 for block ratio calculation). Generally, Cu (II) can form 4, 5 or 6 coordinated complexes

13 with a wide range of ligands. However, because of steric hindrance issues, a mixture of

14 lower coordination numbers will be produced in general[32]. Therefore, the maximum

15 micelle loading at 1:1 ratio should be a combination of Cu (II) coordination and the

16 copper ions dissolved in the core of P4VP-PEG-P4VP SCRMs, which was revealed by

17 TEM in ESI Figure S8a.

18 The coordination of the Cu (II) can be confirmed directly by EPR in DMSO. When

19 measured at room temperature, the EPR peaks of $CuCl_2$ were not clearly separated

20 (Figure 3a). Therefore, the temperature was adjusted to 108 K to improve Cu (II)

21 signals. As shown in Figure 3b and c, $g_{//}=2.3593$ and $g_{\perp}=2.0906$ were observed for Cu

22 (II), and $g_{//}=2.4050$ and $g_{\perp}=2.0914$ for the complexes of $CuCl_2$-(P4VP-PEG-P4VP).

23 These indicated the presence of copper (II) d^9 paramagnetic species in this system as

24 expected. Similar EPR behavior was observed on Cu/P4VP[39], which validated that the

25 copper ions were indeed located in the P4VP-PEG-P4VP SCRMs.

26 $CuCl_2$-(P4VP-PEG-P4VP) SCRMs were used as catalysts in for TMP **1** oxidized to

27 trimethyl-p-benzoquinone (TMBQ) **2** by dioxygen (Table 1). Generally, the reaction

28 also produces 4-chloro-2,3,6- trimethylphenol (CTP) **3** and

29 2,2-3,3-5,5-hexamethyl-4,4-biphenyldiol (HBD) **4** in the process, as detectable

30 compounds by GC. The control experiment without the catalyst, did not proceed to any

31 appreciable extents (Table 1, Run 1). Due to the important role that H_2O played in the

32 oxidation, reaction could proceed with addition of a small amount of water (Table 1,

1   Run 2-3). Then, the oxidation of **1** with CuCl$_2$-P4VP and CuCl$_2$-(P4VP-PEG-P4VP)

2   (Cu: 4VP = 1:1) were carried out under similar conditions (Table 1, Run 4 and 6). After

3   24 h, only a low yield of **2** was obtained with CuCl$_2$-P4VP, indicating a much higher

4   activity of CuCl$_2$-(P4VP-PEG-P4VP). It was suggested that the hydrophilic segments

5   and the core domain containing water had a positive effect on the oxidation. The water

6   pool could dissolve more copper ions, so that the catalytic centers are concentrated and

7   the catalyst became harder to wash off. The mesoscale structure of the SCRM decreased

8   the entropy of reaction by reducing distances among the substrates, catalytic centers and

9   H$_2$O, resulting in efficient catalytic activity for this reaction.

10   The time course of the oxidation of TMP **1** with CuCl$_2$-(P4VP-PEG-P4VP) was

11   shown in Figure 4. With the substrate TMP **1** being consumed, the CTP **3** appeared at

12   first, and finally changed to the TMBQ **2**. A small amount of the HBD **4** was detected

13   after the formation of **2**. The reaction system essentially induces many competitive

14   reactions, such as C–C and C–O coupling and peroxide formation from phenoxy

15   radicals and dioxygen. Thus, the yield and selectivity of **2** are very sensitive to the

16   reaction conditions, particularly to the molar ratio of 4VP to CuCl$_2$. At low ratio, the

17   results were unsatisfactory (Table 1, Run 5). Higher copper loading in the ligand

18   increased the conversion of **1** (Table 1, Run 6-8). This oxidation reaction at a relatively

19   high temperature will produce a series of higher multimers (hard to be completely

20   detected by GC). After the conversion reached 100%, although the yield of **2** was not

21   high (Table 1, Run 6), the selectivity of **2** increased with copper loading increase.

22   With a low cross-linking extent of P4VP-PEG-P4VP RMs, the corresponding

23   catalysts usually cannot be used more than twice, owing to its mechanical degradation

24   and/or elution of the catalyst. However, this limitation can be overcome by increasing

25   the cross-linking content[25]. Therefore, as a better reaction condition compared to the one

26   using non-cross-linked CuCl$_2$-(P4VP-PEG-P4VP) as catalyst, the reaction was repeated

27   using 30% cross-linking content of the CuCl$_2$-(P4VP-PEG-P4VP) (Table 2) for five

28   times. After being thoroughly dried and treated with nitric acid, the amount of copper in

29   the catalyst was measured by atomic absorption spectroscopy (AAS). The amount of

30   copper in the non-cross-linked CuCl$_2$-(P4VP-PEG-P4VP) declined significantly. In the

31   third reaction, only 52.7% copper was left and the yield obviously decreased, which was

32   due to the destruction in the multiple trials at high temperature. The results of 30%

1   cross-linked $CuCl_2$-(P4VP-PEG-P4VP) show that the catalyst could be easily recovered

2   and reused without great decrease of the activity. The copper was proved to remain in

3   the catalyst (by the ratio of copper/P4VP-PEG-P4VP), without much loss after every

4   recycle. After the fifth reaction, the remaining copper just dropped to 63.3%, at the

5   same level with non-cross-linked $CuCl_2$-(P4VP-PEG-P4VP). The Recycle 2~4 (Table 2)

6   brought about reasonable decreases in reaction yields. In the second recycle **2** yielded

7   higher percentage than in the first one, might due to the absorption of SCRMs catalyst

8   carrier and the redistribution of copper in first reaction. Additionally, the change in

9   morphologies of $CuCl_2$-(P4VP-PEG-P4VP) was investigated in ESI Figure S8.

10

11   **Conclusion**

12   In this study, a novel catalytic system for oxidation reaction of TMP was designed

13   and synthesized. Firstly an amphiphilic block copolymer P4VP-PEG-P4VP was

14   synthesized via the anionic polymerization technique. After being added into

15   water/1-hexanol mixed solution, the block copolymer P4VP-PEG-P4VP self-assembled

16   into reverse micelles. The reverse micelles consisted of a hydrophobic shell of P4VP

17   and a hydrophilic core of PEG, partly with a water pool in the core. Demonstrated by

18   TEM and ζ potential, the structure and morphologies of the reverse micelles changed

19   along with the pH of surroundings. To stabilize the structure, BIEE was used to

20   cross-link the shell by quarternizing the nitrogen atoms on the pyridine groups. SCRMs

21   were reinforced through covalent bonds between P4VP chains, to maintain the structure

22   whenever the environmental conditions changed.

23   After coordinating with copper ions, the $CuCl_2$-(P4VP-PEG-P4VP) SCRMs complex

24   was obtained as a kind of catalyst. The oxidation of TMP used the catalyst system with

25   dioxygen under ambient pressure. Taking advantage of the coordination with metal ions,

26   the distribution of metal catalytic active centers in the structure, and the co-catalysis

27   effect of the immobilized water droplets, $CuCl_2$-(P4VP-PEG-P4VP) demonstrated an

28   efficient catalytic activity and recoverability. It is indicated that the designed polymeric

29   catalyst carrier has the potential to provide a more reactive and recoverable catalytic

30   system for catalytic oxidation.

31

32

Acknowledgement

## References

1. Y. He and C. Cai, *Chem. Commun.*., 2011, **47**, 12319-12321.

2. B. Saha, D. Gupta, M. M. Abu-Omar, A. Modak and A. Bhaumik, *J. Catal.*, 2013, **299**, 316-320.

3. Y. Zhang and S. N. Riduan, *Chem. Soc. Rev.*, 2012, **41**, 2083-2094.

4. B. L. Moore, A. Lu, D. A. Longbottom and R. K. O'Reilly, *Polym. Chem.*, 2013, **4**, 2304-2312.

5. H. Ma and J. Hao, *Chem. Soc. Rev.*, 2011, **40**, 5457-5471.

6. B. L. Moore, D. Moatsou, A. Lu and R. K. O'Reilly, *Polym. Chem.*, 2014, **5**, 3487-3494.

7. S. Zhang and Y. Zhao, *ACS nano*, 2011, **5**, 2637-2646.

8. D. Trong On, D. Desplantier-Giscard, C. Danumah and S. Kaliaguine, *Appl. Catal., A*, 2001, **222**, 299-357.

9. H. Sun, K. Harms and J. Sundermeyer, *J. Am. Chem. Soc.*, 2004, **126**, 9550-9551.

10. W. Brenner, (Hoffman-La Roche), *Ger. Pat.*, 2,221,624, 1972.

11. (BASF AG), *Eur. Pat. Appl.*, EP 475,272 A2, 1992.

12. T. Isshiki, T. Yui, H. Uno, M. Abe, (Mitsubishi Gas Chemical Co.), *Eur. Pat.*, 0,127,888, 1984.

13. K. Takehira, M. Shimizu, Y. Watanabe, H. Orita and T. Hayakawa, *J. Chem. Soc., Chem. Commun.*, 1989, 1705-1706.

14. K. Takehira, M. Shimizu, Y. Watanabe, H. Orita and T. Hayakawa, *Tetrahedron Lett.*, 1989, **30**, 6691-6692.

15. M. Shimizu, Y. Watanabe, H. Orita, T. Hayakawa and K. Takehira, *Bull. Chem. Soc. Jpn.*, 1992, **65**, 1522-1526.

16. K. Feng, M. L. Peng, D.H. Wang, L.P. Zhang, C.H. Tung and L.Z. Wu, *Dalton T.*, 2009, 9794-9799.

17. K. Takaki, Y. Shimasaki, T. Shishido and K. Takehira, *Bull. Chem. Soc. Jpn.*, 2002, **75**, 311-317.

18. S. Klingelhöfer, W. Heitz, A. Greiner, S. Oestreich, S. Förster and M. Antonietti, *J. Am. Chem. Soc.*, 1997, **119**, 10116-10120.

19. P. Khullar, A. Mahal, V. Singh, T. S. Banipal, G. Kaur and M. S. Bakshi, *Langmuir*, 2010, **26**, 11363-11371.

20. Y. Liu, V. Piñón and M. Weck, *Polym. Chem.*, 2011, **2**, 1964-1975.

21. L. K. Shrestha, R. G. Shrestha, M. Abe and K. Ariga, *Soft Matter.*, 2011, **7**, 10017-10024.

22. R. K. O'Reilly, in *Supramolecular Chemistry*, John Wiley & Sons, Ltd, 2012.

23. A. Vavasori, L. Ronchin and L. Toniolo, *Appl. Catal., A*, 2010, **389**, 108-113.

24. A. Vavasori, L. Ronchin, E. Amadio, L. Toniolo and G. Cavinato, *J. Mol. Catal. A: Chem.*, 2009, **299**, 5-11.

25. H. M. Jung, K. E. Price and D. T. McQuade, *J. Am. Chem. Soc.*, 2003, **125**, 5351-5355.

26. L.C. Lee and Y. Zhao, *Org. Lett.*, 2012, **14**, 784-787.

27. L.C. Lee and Y. Zhao, *ACS Catal.*, 2014, **4**, 688–691.

28. S. P. Anthony and J. K. Kim, *Chem. Commun.*, 2008, 1193-1195.

29. H.D. Koh, M. Changez and J.S. Lee, *Macromol. Rapid Commun.*, 2010, **31**, 1798-1804.

30. M. Zhang, L. Rene-Boisneuf, Y. Hu, K. Moozeh, Y. Hassan, G. Scholes and M. A. Winnik, *J. Mater. Chem.*, 2011, **21**, 9692-9701.

31. N. A. Rahim, F. Audouin, B. Twamley, J. G. Vos and A. Heise, *Eur. Polym. J.*, 2012, **48**, 990-996.

32. T. Lin, C.L. Li, R.M. Ho and J.C. Ho, *Macromolecules*, 2010, **43**, 3383-3391.

33. B. K. Kuila, M. S. Rama and M. Stamm, *Adv. Mater.*, 2011, **23**, 1797-1800.

34. A. J. Pardey and C. Longo, *Coord. Chem. Rev.*, 2010, **254**, 254-272.

35. M. Vamvakaki, N. Billingham and S. Armes, *Macromolecules*, 1999, **32**, 2088-2090.

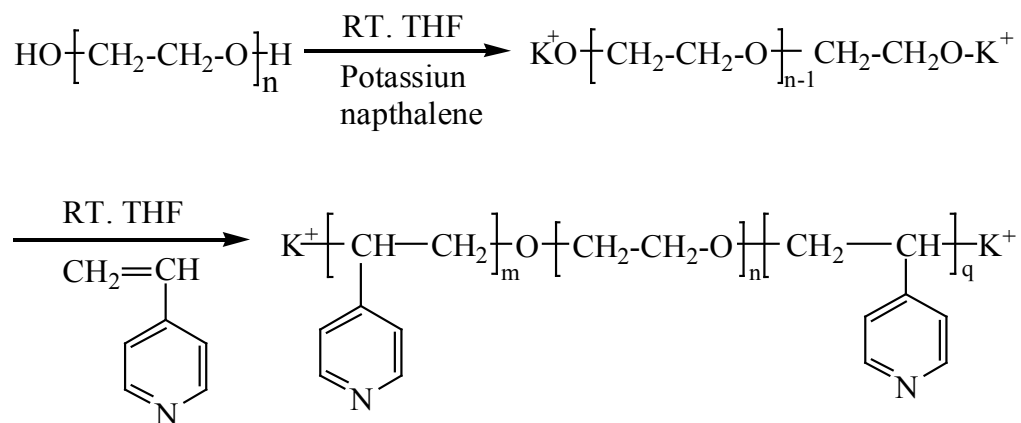36. R. W. O'Brien and R. J. Hunter, *Can. J. Chem*, 1981, **59**, 1878-1887.

1 37. L. Luo and A. Eisenberg, *Angew. Chem.*, 2002, **114**, 1043-1046.

2 38. R. Vyhnalkova, A. H. Mueller and A. Eisenberg, *Langmuir*, 2014.

3 39. A. J. Pardey, A. D. Rojas, J. E. Yanez, P. Betancourt, C. Scott, C. Chinea, C.

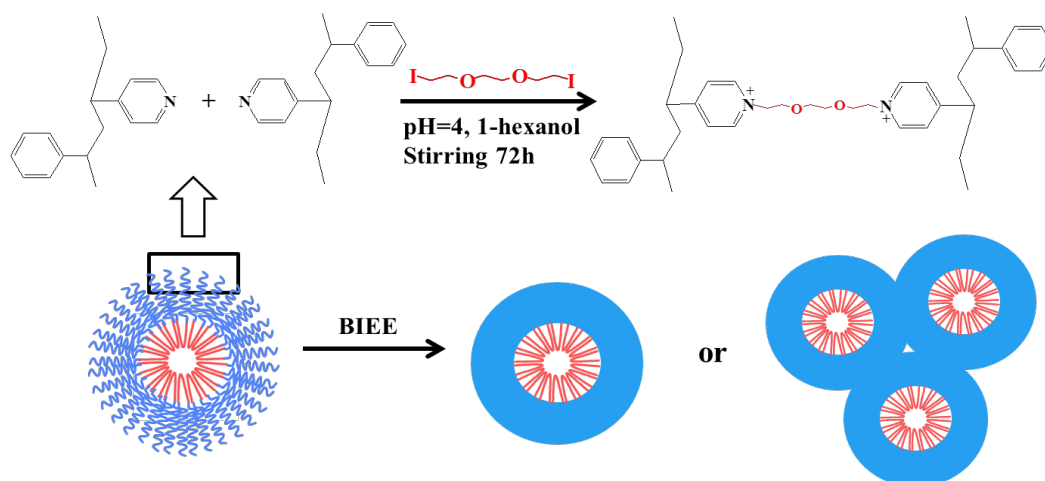4   Urbina, D. Moronta and C. Longo, *Polyhedron*, 2005, **24**, 511-519.

5

6
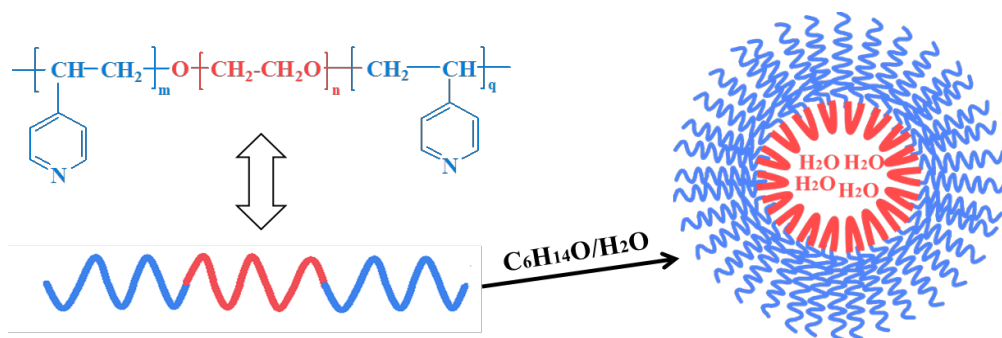
1

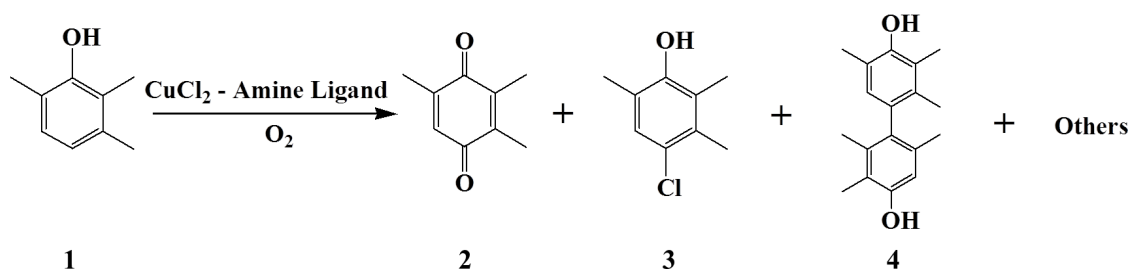2 **Scheme 1.** Structure of the amphiphilic block copolymer P4VP-PEG-P4VP reverse

3 micelles in 1-hexanol/water mixed solution.

$$HO\text{-}[CH_2\text{-}CH_2\text{-}O]_n\text{-}H \xrightarrow[\substack{\text{Potassiun} \\ \text{napthalene}}]{\text{RT. THF}} \overset{+}{K}O\text{-}[CH_2\text{-}CH_2\text{-}O]_{n\text{-}1}\text{-}CH_2\text{-}CH_2O\text{-}K^+$$

$$\xrightarrow[\substack{CH_2=CH}]{\text{RT. THF}}$$

$$K^{\pm}\text{-}[CH\text{-}CH_2]_m\text{-}O\text{-}[CH_2\text{-}CH_2\text{-}O]_n\text{-}CH_2\text{-}CH]_q\text{-}K^+$$

Scheme 2. The synthesis of the P4VP-PEG-P4VP block copolymer.

Scheme 3. The inter-micellar and intra-micellar cross-linking of PEG-P4VP-PEG RMs by BIEE.

Table 1. Oxidation of TMP with CuCl$_2$-Amine Ligand.

Reaction scheme showing compounds **1**, **2**, **3**, **4** + Others

Run	Amine Ligand[a] (mmol)	CuCl$_2$[b] mol %	H$_2$O[c] mol %	Conv. %	Product and Yield/%			Mass balance[d] %
					2	3	4	
1	-	10	0	no reaction	-	-	-	-
2	-	10	100	tr	tr	tr	tr	tr
3	-	10	1000	100	44	17	tr	61
4	P4VP	10	1000	49	3	0	tr	6
5	P4VP-PEG-P4VP	2	1000	39	2	6	7	38
6	P4VP-PEG-P4VP	10	1000	100	46	tr	tr	46
7	P4VP-PEG-P4VP	50	1000	100	62	6	tr	68
8	P4VP-PEG-P4VP	100	1000	100	74	7	tr	81

Reaction Conditions: **1** (1 mmol), 1-hexanol (20 mL), O$_2$ (1 atm, pure oxygen bubbled in from a gas cylinder), reaction time (24 h), 90 °C.

[a] Ratio of 4VP unit of P4VP to CuCl$_2$ is unity.

[b,c] Based on **1**.

[d] Total yield of **2,3,4**.

Table 2. Recycle of catalyst $CuCl_2$-(P4VP-PEG-P4VP) in the oxidation of TMP.

Catalyst	Recycle	$CuCl_2$	Conv.	Product and Yield/%			Mass balance[a]
		mol%	%	2	3	4	%
Non-cross-linked $CuCl_2$-(P4VP-PEG-P4VP)	First	100[b]	100	78	5	3	86
	Second	68.4	100	66	tr	2	68
	Third	52.7	98	57	tr	2	60
30% cross-linked $CuCl_2$-(P4VP-PEG-P4VP)	First	100	100	74	7	tr	81
	Second	95.9	100	88	2	8	98
	Third	83.3	100	87	3	4	94
	Forth	81.6	100	79	7	1	86
	Fifth	63.3	100	68	tr	1	69

Reaction Conditions: **1** (1 mmol), 1-hexanol (20 mL), O_2 (1 atm), reaction time (24 h), 90 °C. Ratio of H_2O to $CuCl_2$ is 10 in the first reaction, and the amount is fixed in following reactions.

[a] Total yield of **2,3,4**.

[b] Ratio of 4VP unit of P4VP to $CuCl_2$ is 1 in the first reaction.
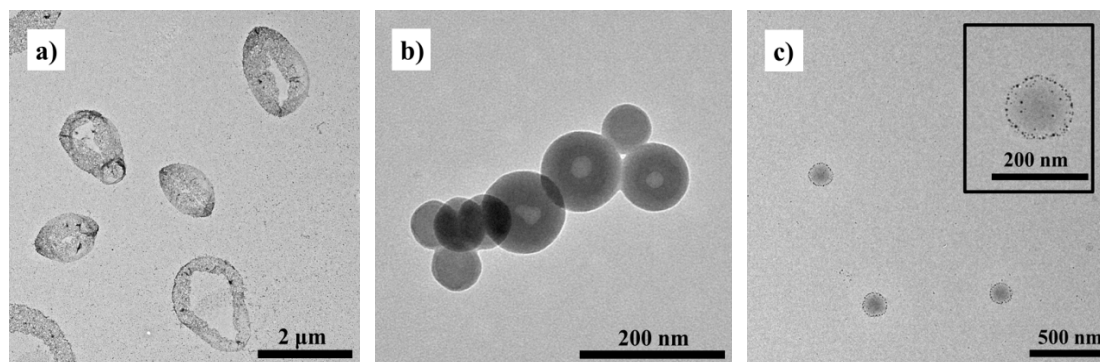
Figure 1. TEM images of a) PEG-P4VP, b) P4VP-PEG-P4VP reverse micelles in mixed solution and c) with 5 mol % CuCl$_2$ added into mixed solution (polymer weight: 0.15 %, mass ratio of 1-hexanol/water = 1).
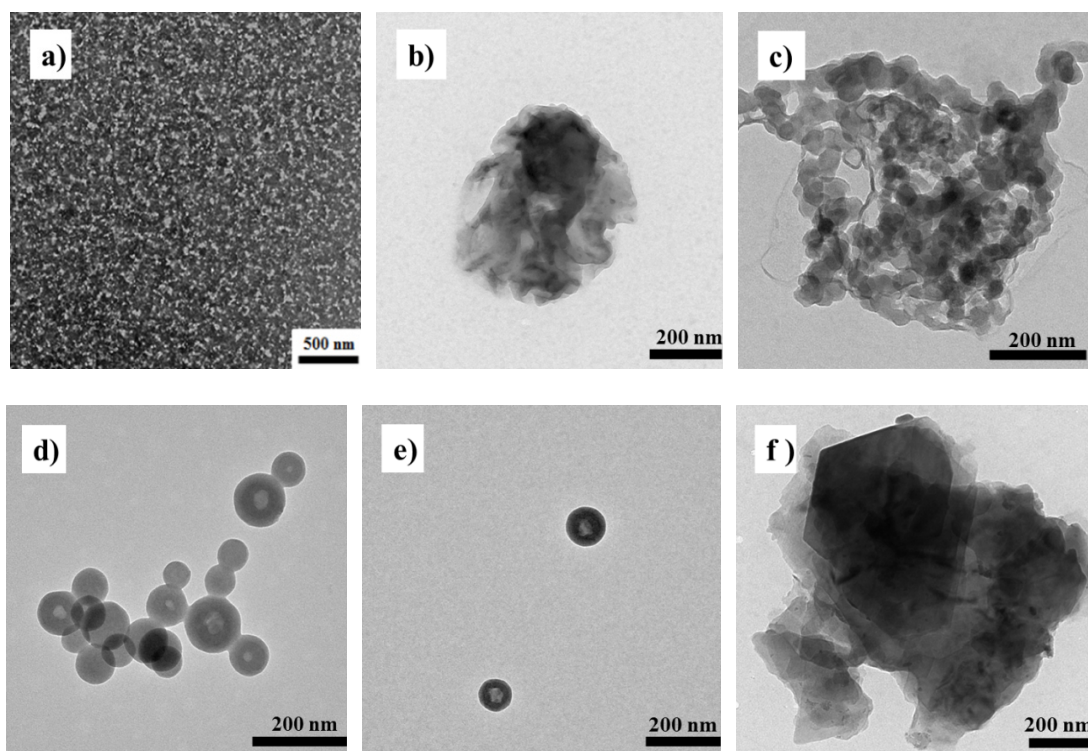
Figure 2. TEM images of P4VP-PEG-P4VP self-assemblies prepared in a mixture solution of water/1-hexanol: a) 100% 1-hexanol, b) 80% 1-hexanol + 20% water, c) 60% 1-hexanol + 40% water, d) 40% 1-hexanol + 60% water, e) 20% 1-hexanol + 80% water, f) 100% water. (polymer weight: 0.15%)
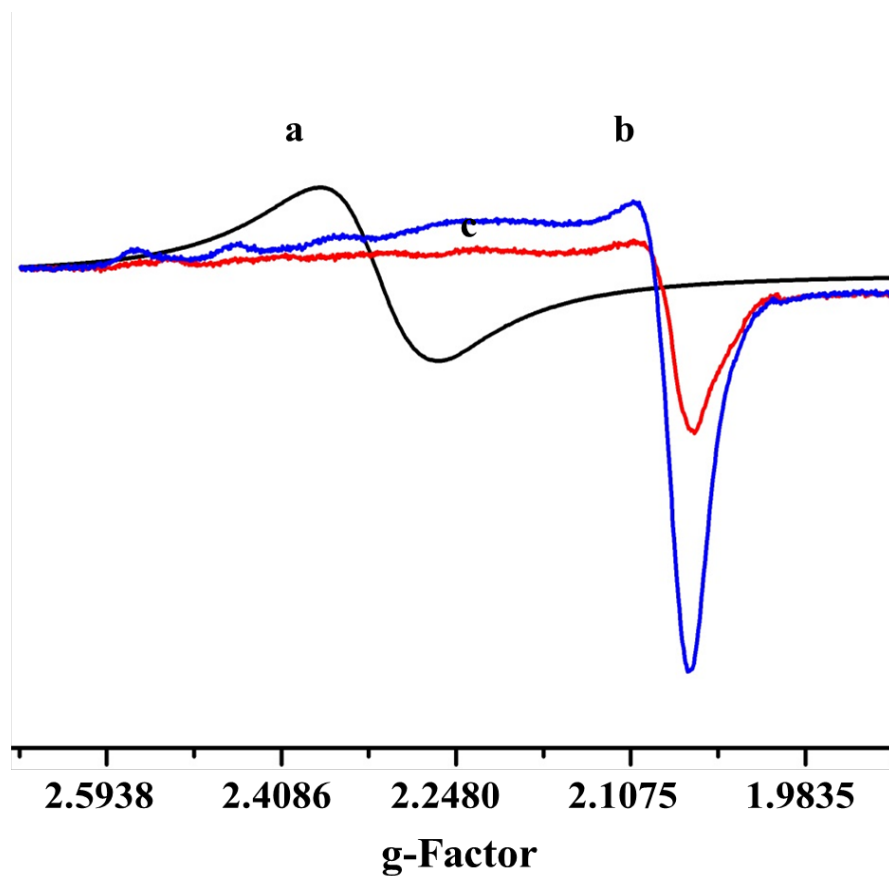
Figure 3. X-band EPR spectra in the 2.6976~1.9274 g-Factor region of: a) $CuCl_2$ at room temperature, b) $CuCl_2$ at 108 K and c) $CuCl_2$-(P4VP-PEG-P4VP) at 108 K in DMSO.
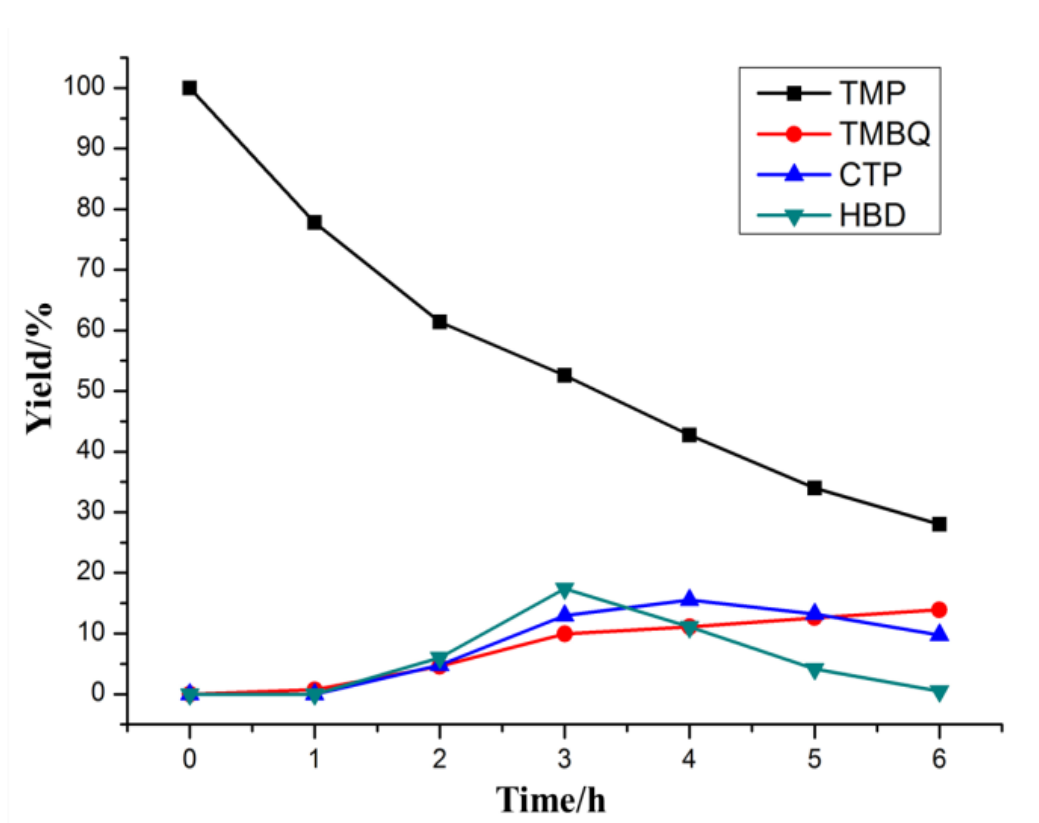
Figure 4. Oxidation of TMP with CuCl$_2$-(P4VP-PEG-P4VP). Conditions see: Run 6 in Table 1.